

Magnetic effects of defect pair formation in ZnO

W A Adeagbo¹, G Fischer¹, A Ernst² and W Hergert¹

¹ Institute of Physics, Martin Luther University Halle-Wittenberg, Von-Seckendorff-Platz 1, D-06120 Halle, Germany

² Max Planck Institute of Microstructure Physics, Weinberg 2, D-06120 Halle, Germany

E-mail: waheed.adeagbo@physik.uni-halle.de

Received 10 July 2010, in final form 12 September 2010

Published 12 October 2010

Online at stacks.iop.org/JPhysCM/22/436002

Abstract

In order to gain insight into the so-called d^0 -magnetic properties of defective ZnO we have carried out first principles calculations on various types of defects formed by intrinsic defects and doped atoms as well as pairs of them. The doped atoms include N and H. In agreement with previous works we find several possibilities to create magnetic defects especially by hole formation. Our results also show that two defects which are in the vicinity of each other and that are magnetic when isolated, in general become non-magnetic if one of them is acceptor-like and the other one donor-like. Furthermore, we have investigated the magnetic interaction of different defect pairs via total energy calculations, the results of which show in all cases the stability of ferromagnetic configurations. In order to reproduce the experimentally found localization of the magnetic hole states we have investigated the effect of applying correlation corrections on the p orbitals containing these holes.

(Some figures in this article are in colour only in the electronic version)

1. Introduction

The search for ferromagnetism in semiconducting materials such as ZnO has attracted considerable attention due to their potential applications in optoelectronic and spintronic devices. After the theoretical prediction of room temperature ferromagnetism in Mn-doped ZnO [1], also ZnO compounds doped with other magnetic transition metal ions such as Fe, Ni, Co [2–5], etc have been undergoing intensive studies. However, it seems that dopants of this kind are not essential for the formation of magnetic order [4, 6–8] since their interaction is too weak. Instead non-magnetic dopants such as carbon [9, 10], nitrogen [11–13] or even argon [14] have led to ferromagnetic (FM) ZnO samples as well. This wide spread of different dopant materials suggests that they are not so much needed as carriers of the magnetic moment inside the samples, but are rather necessary to enable intrinsic lattice defects that are magnetic. Since defects are relatively easily created at interfaces and surfaces most FM ZnO samples have been thin layers. However, FM behaviour has also been detected at bulk ZnO recently [12].

This is supported by density functional theory (DFT) calculations that have also shown that magnetic defects do

not require magnetic dopants in general. Examples for this, not only in ZnO, are cation vacancies [15–17], carbon and nitrogen substitutes [11, 18, 19] or alkali metal substitutes [20]. The magnetic moments in these systems arise from localized holes that form triplet states which have a stable magnetic ground state. This phenomenon is generally known as d^0 magnetism [21], since the magnetic moment (MM) does not arise from d electrons but rather from localized holes in p-bands carrying a magnetic moment. It should be mentioned that recent results involving corrections of systematic errors in the treatment of holes inherent to standard DFT have shown that the magnetic triplet ground state of the p holes might not be robust enough to support FM ordering in the material, as it is only very little lower in energy than the non-magnetic singlet state [22]. But yet, owing to a lack of experimental verification for the former and due to the overwhelming amount of other theoretical and experimental evidence, it is now generally accepted that formally diamagnetic materials, in particular ZnO, do exhibit weak FM behaviour due to intrinsic defects [23] and that this magnetism originates from localized p holes.

The interaction mechanism, on the other hand, is not completely understood yet. From a qualitative point of view

one can say that increasing the hopping integral of the electrons responsible for magnetism increases the interaction range due to a larger delocalization but also reduces the strength of the magnetic moment [11]. It also seems clear that the exchange must be carrier mediated, which is due to its long range. But yet, the exact mechanism remains unclear. Shen *et al* and Peng *et al* [24, 25] have suggested a p–p coupling providing a long-ranged and strong FM interaction which could generally explain the experimentally found d^0 ferromagnetism in diluted magnetic oxides [24, 26, 27]. An oscillatory behaviour of the coupling constants J_{ij} was found as well [28–30] and RKKY interaction has thus been proposed as well and discussed controversially [31–34].

Problems arise again if the corrections to the standard DFT treatment of the holes are applied. The latter, for example, predicts a smearing of the two holes of a cation vacancy around the four nearest oxygen neighbours. In experiment, however, they localize in two p orbitals on two different O atoms, respectively [35]. The systems can therefore be regarded as strongly localized ones, which standard DFT describes rather poorly. Thus, several attempts to improve the description of these p orbitals have been made, for example LDA + U in alkaline earth monoxides [19], self-interaction corrections in MgO [18] and, as already mentioned above, special hole treatment in ZnO [22] were applied. They have, to different extents, reproduced the localization of the holes. However, these corrections have as well led to an insulating character of the investigated samples thus cancelling any magnetic exchange mediated by free electrons.

The aim of this paper is to investigate the formation of magnetic defects and the interaction existing between some of the possible isolated defect pairs in order to give some clues about how the former contribute to d^0 ferromagnetism in ZnO samples observed in experiments. For this we have calculated the magnetic moment induced by single intrinsic defects such as Zn and O vacancies (V_{Zn} and V_{O} , respectively), interstitials (Zn_i and O_i) and substitutional defects such as O_{Zn} and Zn_{O} , where an O atom occupies a Zn site and vice versa, and antisite defects AS in which a nearest neighbour (NN) O and Zn atom have flipped sites. Extrinsic substitutional defects of nitrogen and hydrogen (H) at Zn and O sites (N_{Zn} , N_{O} , H_{Zn} , and H_{O} , respectively), and hydrogen interstitials (H^i) were also considered. The reason for investigating hydrogen is that it has been suggested to play an important role in the formation of magnetism in ZnO [36, 37]. This fact is based on the donor-like character of hydrogen which leads to an increased carrier density [38] again increasing magnetic exchange. In order to see if H directly contributes to d^0 ferromagnetism by forming magnetic defects we have also investigated point defects involving H. We then moved on to investigate the effect of bringing different isolated defects closer together, i.e. single defects forming pairs. We find that certain combinations of single magnetic defects annihilate each other. This on the one hand reduces the chances of introducing magnetism, on the other hand it can help to explain an experimentally found saturation effect of the magnetization [12]. We then calculated the strength of magnetic interaction of some of the magnetic defect pairs. The results of this together with an

investigation of the equilibrium volume change for different defects [12] support the assumption that zinc vacancies play the dominant role in the observed ferromagnetism in defective ZnO. Finally, in order to reproduce the experimentally found localization as mentioned above, we have investigated the effect on the magnetism of applying Hubbard- U corrections on the magnetic p orbitals.

2. Computational details

All our calculations were performed by applying the pseudopotential method based on density functional theory (DFT) in the generalized gradient approximation [39–41]. This was carried out with the Vienna *ab initio* Simulation Package [42, 43] using the projector augmented-wave method [44]. Due to the strong electronic correlations between 3d electrons, standard DFT cannot accurately describe the electronic structure of ZnO. Therefore, we used the GGA + U approximation and applied the on-site Coulomb correlation energy correction $U = 5.7$ eV with a J value of 1.0 eV. The defects in ZnO were simulated with $3 \times 2 \times 2$ supercells of dimensions $9.64 \times 11.12 \times 10.29 \text{ \AA}^3$ containing 96 atoms and built from a conventional orthorhombic unit cell of eight atoms. The expansion of the electronic wavefunctions into plane waves was done using a cut-off energy of 400 eV. For the k -point sampling, a $2 \times 2 \times 2$ mesh within the Monkhorst–Pack special k -point scheme [45] in the Brillouin zone was chosen. Test calculations using up to $4 \times 4 \times 4$ k -points verified that the former k -mesh provides good convergence with respect to total energy differences and magnetic moment formation. The iterative minimization of the charge density was conducted within the framework of the residual minimization direct inversion in the iterative subspace (RMM-DIIS) method [46]. To calculate atomic relaxations we used the gradient quasi-Newton method. We assumed that the convergence was achieved when the forces acting on the atoms did not exceed $0.001 \text{ eV \AA}^{-1}$. With the above settings the calculated lattice constants of $a = 3.245 \text{ \AA}$ and the c/a ratio of 1.603 are comparable to the experimental values (3.249 \AA and 1.602, respectively [47]). The band gap obtained is of the order of 1.35 eV, which is still a lot smaller than the experimental value of 3.43 eV, but large enough to describe magnetic interaction adequately and, furthermore, comparable to previous first principles investigations [48].

In some cases we use the formation energy of certain defects in our discussion. For neutral defects it is calculated via [48]

$$E_i[X] = E^{\text{tot}}[X] - E^{\text{tot}}[\text{Host}^{\text{perfect}}] - \sum_i n_i \mu_i, \quad (1)$$

where $E^{\text{tot}}[X]$ is the total energy of the supercell containing the defects X , $E^{\text{tot}}[\text{Host}^{\text{perfect}}]$ is the total energy of the corresponding supercell without defects, n_i is the number of atoms removed or added, and μ_i is the chemical potential of the corresponding atoms which depends on the experimental growth conditions. For the calculation of μ_i for oxygen, hydrogen and nitrogen atoms we chose O_2 , H_2 and N_2

molecules, respectively, while the solid hexagonal close-packed phase was chosen for Zn. Our calculated value for the formation energy for ZnO, -3.7 eV, is in good agreement with -3.6 eV from experiment [49]. For further technical details on such calculations see, for example, [48].

To estimate the Curie temperatures for certain magnetic systems Monte Carlo (MC) simulations were performed. For a short summary of this technique as it was performed in this work we refer the reader to a paper [50] in which it was applied as well. To represent the defect systems in the present work ZnO lattices were constructed. In order to avoid finite-size effects their size was varied from $26 \times 26 \times 26$ to $30 \times 30 \times 30$ ZnO single unit cells. In these lattices the defects were randomly distributed having a concentration of 4.17% in the respective sublattice, i.e. O or Zn. The value of 4.17% defects in one sublattice corresponds to two defects in the 96 atom supercell. Averaging of the magnetization and inner energy was done over 20 000 MC steps after thermal equilibrium was achieved. The latter was assumed to be reached after 10 000 lattice sweeps. The convergence with respect to these two numbers of performed MC steps was carefully checked. For importance sampling the Metropolis algorithm was used. This procedure was carried out for 20 different random defect distributions, over which again averaging of the measured quantities was done. The Curie temperatures were extracted from the fourth-order cumulant [51].

3. Results and discussion

3.1. Single defects

To investigate the magnetic moments induced by single defects a supercell of $3 \times 2 \times 2$ orthorhombic unit cells as discussed above was used. The nearest neighbour atoms around the defect were relaxed. The total magnetic moments per supercell for single O and Zn vacancies (V_O and V_{Zn} , respectively) and a single N or H atom substituting O or Zn lattice sites ($(N/H)_{(O/Zn)}$) are reported in table 1. The defects were chosen regardless of their formation energies, since all possibilities concerning magnetic properties are formally of interest. We can see that the acceptor-like defects V_{Zn} , O_{Zn} and N_O intrinsically induce magnetic moments of values 1.89, 1.96 and $0.99 \mu_B$, respectively. It should be noted that the non-integer magnetic moments arise when the systems are relaxed, unrelaxed defect systems always have integer values. For N_O the largest contribution comes from nitrogen ($\approx 0.35 \mu_B$), which can be seen in figure 1. Also shown there are the contributions from first nearest neighbours (NN) Zn ($\approx 0.15 \mu_B$) and oxygen ($\approx 0.23 \mu_B$) being smaller. For V_{Zn} the largest contribution of the local moment comes from the 2p orbitals of its NN oxygen atoms. As can be seen from figure 1 this is $\approx 0.90 \mu_B$. The contribution from NN Zn and second NN O atoms are small. What one can see, however, is that for both defect kinds the magnetization does not monotonically go to zero with increasing neighbour distance. For V_{Zn} , this is very pronounced for the O atoms, for which the magnetization has two clear local maxima. For N_O one can clearly see a maximum for each atom kind, O and

Table 1. Listed below are the magnetic moments of the investigated single defects after structural relaxation. H^i is an interstitial H atom. $(N-H)_{O/Zn}$ represents the nitrogen-hydrogen complex [52, 53] at the O or Zn site. The case of 0.00 means that not only the net magnetization of the whole cell sums up to zero, but that there is no magnetization present anywhere in the cell.

Defect	MM (μ_B)	Defect	MM (μ_B)	Defect	MM (μ_B)
V_{Zn}	1.89	V_O	0.00	H^i	0.00
H_{Zn}^a	1.03	H_O^b	0.00	$(N-H)_O$	0.00
N_{Zn}^c	1.00	N_O	0.99	$(N-H)_{Zn}^d$	0.05
O_{Zn}	1.96	Zn_O	0.00	AS	1.99
Zn^i	0.00	O^{ic}	0.00		

^a H forms an O-H bond with one of the neighbouring O atoms.

^b H remains at the former O site.

^c N slightly moves towards one of the NN O.

^d N slightly moves towards the NN O that is closest to the H atom.

^e This refers to the energetically preferred split interstitial configuration in which the interstitial O shares a site with a host O atom. An octahedral or tetrahedral configuration is in fact magnetic but higher in energy, as was also shown before in [54].

Zn, respectively. We should mention that test calculations with larger supercells yielded the same distributions of the magnetic moment. Therefore, we can assume that we are not dealing with a supercell effect.

In the case of O_{Zn} the magnetic moment is almost completely located at the substitutional O atom and its four nearest O neighbours. Contrary to N_O and V_{Zn} there is nearly no magnetization at further atoms. The same holds for the antisite (AS), where the O atom at the Zn site and its three NN (the fourth one being occupied by the Zn atom) carry nearly all of the induced moment of $1.99 \mu_B$.

In several experiments hydrogen related defects in ZnO were found [35, 55]. Therefore, we also investigated several kinds of single defects involving H in order to see if they can form magnetic moments and contribute to ferromagnetism. However, it turns out that this is usually not the case and that instead H atoms sometimes actually tend to reduce any magnetization. This is also shown in table 1. There one sees that only H at a Zn site is a magnetic defect with a moment of $1.03 \mu_B$, which, however, could be interpreted as a reduction of V_{Zn} . An explanation for this can be found in section 3.2.

3.2. Defect pairs

To investigate the magnetic properties of magnetic defect pairs two single defects were placed at several large distances in the supercell, the periodicity of which of course was considered. The resulting stable magnetic moments of such pair defects are summarized in figure 2. One might naively expect them to be added. This, however, does not occur. Instead one sees that in general acceptors (for example V_{Zn} and N_O) and donors (for example N_{Zn} , H) annihilate each other in terms of magnetic moment formation, as the magnetic hole states are occupied by the donated electrons. Examples for this are $V_{Zn}V_O$ and $N_{Zn}N_O$. On the other hand, in the case of two acceptor-like, such as $V_{Zn}V_{Zn}$ and $N_O N_O$, or two donor-like defects, such as $N_{Zn}N_{Zn}$, the obtained total moment for the pair defects is the sum of the single defects. These pairs are

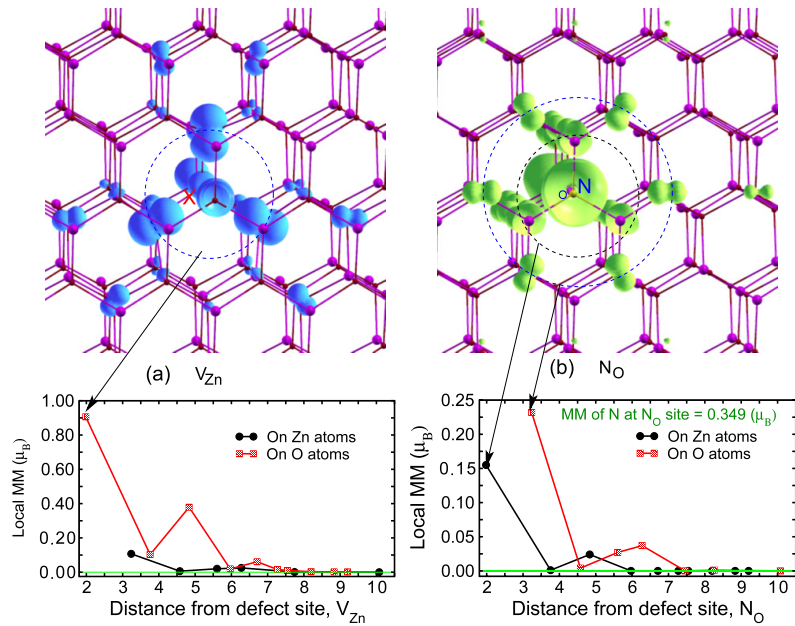


Figure 1. Spin density distribution viewed along the z -axis in the top row and MM distribution in the bottom row for (a) V_{Zn} and (b) N_O . In both cases the magnetic moment induced in the first nearest neighbouring (NN) atoms of the defect site is relatively large. For N_O , the largest contribution by nitrogen ($\approx 0.349 \mu_B$, marked by N_O) is followed by the first NN O atoms shell ($\approx 0.230 \mu_B$) and first NN Zn atoms shell ($\approx 0.15 \mu_B$) as shown in the corresponding lower plot. For V_{Zn} , the largest contribution of the local moment comes from the p orbital of the first NN oxygen atoms around the V_{Zn} marked by X ($\approx 0.90 \mu_B$) while the contributions from Zn and O atoms in the next neighbours are too small (see the corresponding plot below).

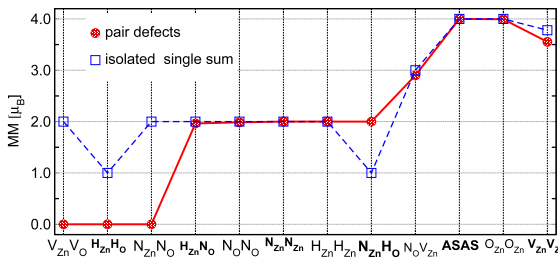


Figure 2. Comparison between total magnetic moment of several pair defects and the sum of the magnetic moments of their two respective single defects.

favourable for forming FM ordering in the material, as they introduce relatively large and stable magnetic moments that may be capable of interacting with other magnetic defects.

The $V_{Zn}V_O$ pair is a nice example for the annihilation effect of a donor-like and an acceptor-like single defect. In order to understand this from an electronic point of view, the projected DOS for the $V_{Zn}V_{Zn}$ and the pair vacancy $V_{Zn}V_O$ defect pairs are shown in figure 3. As it is known, the main source of the magnetic moment for the V_{Zn} defect arises from the two holes in the 2p-band at the O sites surrounding the Zn vacancy [15, 16]. This can be seen in figure 3 at the top, where the partial DOS per atom of the double zinc vacancy is equivalent to that of the single one. With the introduction of the oxygen vacancy two additional electrons are present in the system as V_O is known to be a donor. These annihilate the holes in the oxygen p-bands around the Zn vacancy. One can clearly see the symmetric DOS of the up and down states for $V_{Zn}V_O$ in figure 3.

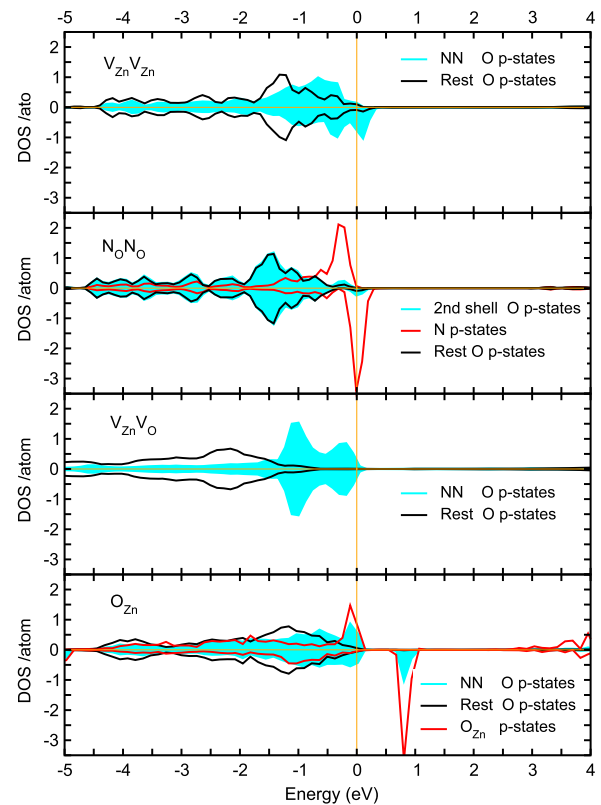


Figure 3. Projected electronic density of states per atom for the following defects (from top to bottom): $V_{Zn}V_{Zn}$, $N_O N_O$, $V_{Zn}V_O$ and O_{Zn} . Not shown are the contributions of the Zn d electrons, since neither do they contribute to magnetism significantly as can be seen from figure 1, nor should they be responsible for the magnetic exchange due to their strong localization.

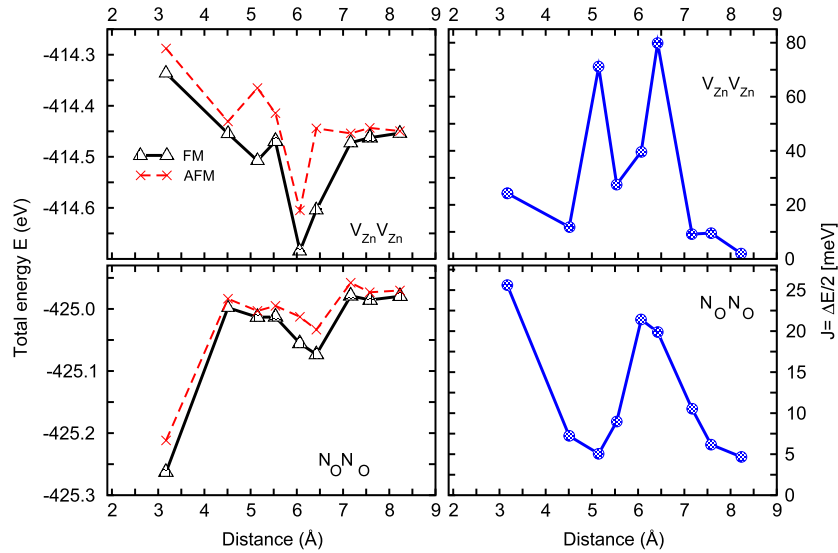


Figure 4. Total energy versus distance d calculation for FM and AFM structure of the defect pairs (left) and resulting magnetic coupling constant J versus d (right).

In most of our pair defect calculations the distant pairs have larger formation energies than the nearest neighbour ones. However, for the favourable pairs $N_O N_O$ (cf figure 4) and $N_O V_{Zn}$ these differences are small. We can therefore assume that clustering of the respective defects does not occur, which otherwise would prevent the formation of interacting defect pairs. In particular, this is also true for $V_{Zn} V_{Zn}$ where the formation energy for forming distant pairs is even slightly lower than that for forming neighbouring pairs, as can be seen from figure 4 as well.

3.3. Magnetic interaction

The magnetic interaction was studied quantitatively for certain defect pairs with stable magnetic moments. These are $V_{Zn} V_{Zn}$, $O_{Zn} O_{Zn}$, $N_O N_O$, $N_O V_{Zn}$ and the AS pair, ASAS. We omitted $H_{Zn} H_{Zn}$ and $H_{Zn} N_O$ since the H atoms tend to migrate through the material due to the relatively low energy barrier. Furthermore, these configurations might be regarded as weakened $V_{Zn} V_{Zn}$ and $V_{Zn} N_O$, respectively, where an H atom is located at the vacancy site. $N_{Zn} N_{Zn}$ is not considered because N atoms tend to occupy O instead of Zn sites. The latter is obtained from calculations of the formation energy, equation (1), which yield $E_f[N_{Zn}] - E_f[N_O] = 1.6$ eV under Zn-rich and O-poor conditions and 4.7 eV vice versa. And as mentioned before for the $N_{Zn} H_O$ pair the magnetic moment is concentrated at one place, which is around the N atom.

To quantify the interaction between such defect pairs we calculated Heisenberg exchange parameters J_{ij} and, thus, mapped it onto a Heisenberg Hamiltonian of the kind

$$H = - \sum_{\langle i, j \rangle} J_{ij} \vec{e}_i \cdot \vec{e}_j, \quad (2)$$

where $\langle i, j \rangle$ denotes interacting pairs and \vec{e}_i is the spin vector of length one. The latter means that the magnitude of the magnetic moment is contained in the J_{ij} . These J_{ij} are

obtained by calculating the total energy differences between FM and AFM alignments of these pairs for distance d ,

$$J(d) = \frac{\Delta E^{\text{mag}}(d)}{2} = \frac{E_{\text{AFM}}(d) - E_{\text{FM}}(d)}{2}, \quad (3)$$

and averaging over each shell, i.e. equidistant defect pairs. The factor 1/2 corresponds to the Hamiltonian in equation (2).

The results for the energy differences against the distance for $V_{Zn} V_{Zn}$ and $N_O N_O$ are shown in figure 4. We can see from these plots that both pair defects generally favour the FM configuration. A strong FM behaviour is shown by the $V_{Zn} V_{Zn}$ pairs. The long range of the interaction can probably be explained by a coupling of the oxygen p orbitals as suggested by Shen *et al* and Peng *et al* for defective ZnO [24, 25]. The reason for the rather unexpected strengthening of the interactions for larger distances can be found in the graphs in figure 1. The interaction between the defects at sites i and j is directly connected to the magnetization at site j induced by defect i and vice versa.

For $N_O N_O$ the interaction is a lot weaker. This is partly due to the reduced magnetic moments which enter J quadratically (see equation (2)). Another reason is shown in figure 3. There one sees that the hybridization between the main carrier of the magnetic moment, the N p orbitals, and the mediator, the O p orbitals, is much smaller than in the $V_{Zn} V_{Zn}$ system where the main carrier and the mediators are both the oxygen p electrons. For the distances of 3.2 Å and 6.1 Å we get $J = 25.6$ meV and $J = 21.4$ meV, respectively. Keeping in mind the denominator of 2 in equation (3) these values represent a much stronger coupling than those obtained by Shen *et al* who calculated 7 meV and 22 meV for 3.25 Å and 6.14 Å, respectively, without the factor 1/2 [24]. This large disagreement is possibly caused by the application of the Hubbard- U in our work. The latter pushes down the non-magnetic Zn d electrons which thus hybridize less with the mediating O p orbitals, thereby increasing the p orbital mediated interaction. The strong

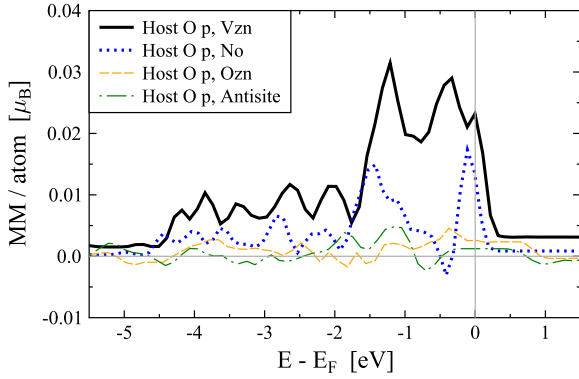


Figure 5. The MM around and below the Fermi level of the p electrons of the host O atoms, i.e. the O atoms not being at the defect sites nor being NN to it. One can clearly see that in the cases of the zinc vacancy and the N substituting O (thick lines) these p electrons are relatively strongly spin polarized up to the Fermi level in contrast to O_{Zn} and the AS (thin lines).

interaction at distances $>6.14 \text{ \AA}$ can be explained in the same way as in the case of $V_{Zn}V_{Zn}$: figure 4 shows that the strength of the J_{ij} is directly related to the distribution of the magnetic moment around the single defects, which is spread far into the host.

Figure 2 shows that the N_OV_{Zn} pair has a stable magnetic moment of $\lesssim 3 \mu_B$. However, during the calculation of the total energies we encountered difficulties in the stabilization of some of the antiparallel alignments. We therefore only mention that the obtained $J(d)$ according to equation (3) are weaker than those for the N_ON_O pairs, but nevertheless the parallel configuration of the magnetic moments always turned out to be the most stable one.

For $O_{Zn}O_{Zn}$ (and the ASAS) we get only very small interaction values of a few meV even for close distances, which can be attributed to the strong localization of the magnetic moment at the central substitutional and the surrounding 4 (3) NN O atoms. This leads to an only very small overlap of their spin polarized p orbitals with those of the p orbitals of the host as is the case for $V_{Zn}V_{Zn}$ and N_ON_O . In figure 3 one can see that the NN O p states of the two latter ones induce spin polarization as well into the rest of the O p electrons of the host. This is not the case for $O_{Zn}O_{Zn}$. To show this more clearly the magnetic moment, i.e. the difference between the up and down spin polarized p states, $MM = N^\uparrow - N^\downarrow$ around and below the Fermi level is depicted in figure 5. These p states are responsible for mediating the magnetic exchange. One can see that those O atoms not being NN to the O_{Zn} carry a much smaller moment ($MM \simeq 0.002 \mu_B$ per atom) than those in the case of V_{Zn} and N_O ($MM \gtrsim 0.02 \mu_B$ and $MM \gtrsim 0.01 \mu_B$ per atom, respectively), which leads to a much weaker ferromagnetic interaction. The same explanation can be applied to the AS pair defect, as the MM of the respective O atoms ($MM \simeq 0.001 \mu_B$ per atom) in the energy region of interest is of the same magnitude as that of O_{Zn} .

We point out that, for $V_{Zn}V_{Zn}$ and N_ON_O as well, some of the configurations obtained at the lower distances are not purely AFM, in fact, they are ferrimagnetic. Nevertheless, short distance interactions do not play a crucial role for the

Table 2. The magnetic moment μ_B on the NN oxygen atoms (O1–O4) around V_{Zn} is shown. Those atoms carrying the localized moments are in none of the cases located along the c axis in agreement with experiment. One can clearly see the growing localization of the magnetic hole states with increasing Hubbard parameter U .

U (eV)	O1	O2	O3	O4
0.0 ^a	0.239	0.238	0.239	0.275
3.0	0.289	0.291	0.289	0.323
7.0	0.554	0.676	0.356	0.110
10.0	0.763	0.773	0.091	0.031
15.0	0.829	0.827	0.046	0.015

^a $U = J = 0.0 \text{ eV}$.

magnetic ordering in the case of diluted magnetic systems. And neither of the AFM and ferrimagnetic configurations is energetically as stable as the FM one.

From the above results one can conclude that, of the considered pairs, the zinc vacancy will mainly contribute to ferromagnetic ordering, since its magnetic interaction is both strong and long-ranged. As mentioned before this agrees well with previous calculations [16, 17, 24] and experimental observations [7, 13] in such ways as suggest V_{Zn} as the main source for d^0 magnetism in ZnO as well. Taking the J_{ij} 's of V_{Zn} from figure 4 and assuming a concentration of $c = 4.17\%$ which corresponds to the concentration of two vacancies in the supercell of 96 atoms we obtain a Curie temperature of $T_C \simeq 60 \text{ K}$. This is clearly below room temperature, despite the very strong interactions. The reason for that is the low concentration of the vacancies which causes the mean distance between the vacancies to be too large for the observed J_{ij} . Keeping in mind that intrinsic charge carriers that are always present in semiconductors like ZnO, but not considered in our calculations, may enhance magnetic interactions, the obtained T_C might still be increased. Of course the question remains whether it could lead to values around room temperature. Performing MC simulations for the N_ON_O system in the same manner, i.e. taking its J_{ij} 's from figure 4 and assuming a defect concentration of 4.17% yields a Curie temperature of around 30 K.

3.4. Correlation corrections of p orbitals

As mentioned earlier standard DFT does not yield the experimentally found localization of the defect-induced hole states. In this paper we tried to reproduce that observation by applying a Hubbard- U onto the p orbitals carrying the holes, i.e. those of the four NN oxygen atoms around the vacancy or those of the N atom. We shall restrict the discussion to V_{Zn} . For the investigation we have kept the Hubbard term $J = 1 \text{ eV}$ constant, whereas U was given the values of 3, 5, 7, 10, 12 and 15 eV, respectively. The resulting distributions of the magnetic moments are given in table 2. One can clearly see that increasing U results in a growing localization on two specific atoms resembling experimental observations [35]. After relaxation the O atoms the holes are localized on are further away (2.21 and 2.17 \AA) from the vacancy centre than the ones unoccupied by holes (2.03 \AA each). This is in good

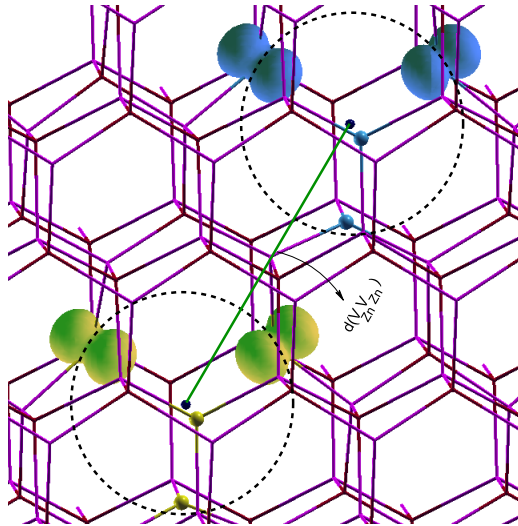


Figure 6. Spin density distribution for the V_{Zn} pair at distance d apart. Here, the correct hole localization leads to magnetic distribution mainly on the two of the farther oxygen atoms around the V_{Zn} while the contribution from the other two oxygen atoms is negligible as is also shown in tables 2 and 3.

Table 3. Given are the exchange parameters J_5 for fifth nearest neighbours V_{Zn} pairs in dependence on the Hubbard- U applied on the surrounding oxygen p orbitals.

U (eV)	0.0 ^a	5.0	7.0	15.0
J_5 (meV)	39.68	55.07	8.51	1.01

^a $U = J = 0.0$ eV.

agreement with previous work [56]. A sketch of the magnetic distribution in the case of two localized holes is shown in figure 6.

It is then of course of interest to explore the behaviour of the magnetic interaction under the influence of an increasing localization. There we find that for low values of U the interaction grows. This is most likely due to the stronger localization of the magnetization while the amount of electrons at the Fermi level remains nearly constant, as can be seen in figure 7. There one sees as well that for Hubbard terms $U \geq 7$ eV a gap opens up and the system becomes insulating. This causes a collapse of the magnetic interaction being mediated by the conduction electrons. The dependence on U for the interaction at a distance of 6.07 \AA , J_5 , is shown in table 3. The collapse of magnetic interaction upon applying correlation corrections [18, 19], in particular reproducing the experimentally found hole localization at two atoms [22], agrees well with previous works.

We mention that the results of the self-consistent calculations for a single defect with the application of large Hubbard- U values on the O p states are very sensitive to the initial conditions. In order to end up with the reported results it is necessary to introduce slightly asymmetric structures around the defects. However, the above results always resemble the energetically lowest solution. We also find that if a pair is introduced this sensitivity is much smaller, as the two defects obviously are sufficient to create the necessary anisotropy in the supercell.

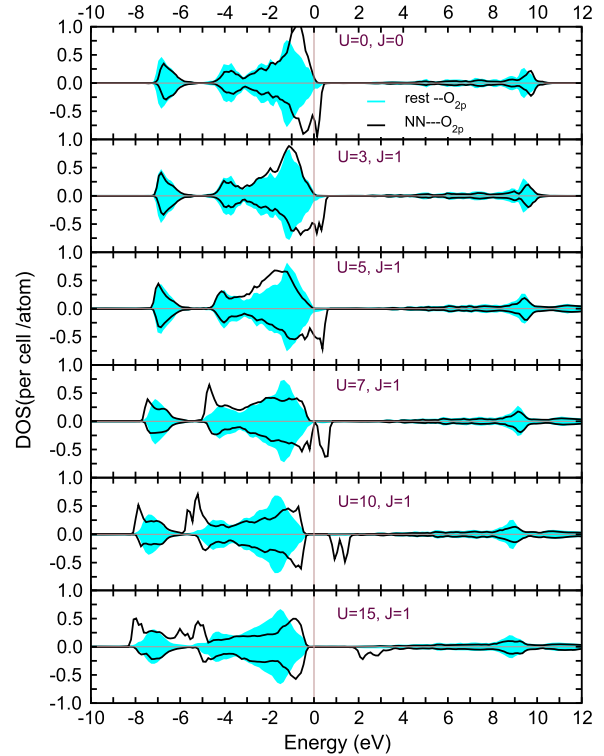


Figure 7. Partial DOSs of the NN oxygen atoms around a Zn vacancy and all other O atoms in dependence on the Hubbard- U . One can see that the increasing U on the NN p states causes a growing energetical separation between the occupied states and the holes which eventually turns the (half-) metallic behaviour of the system into an insulating one.

4. Summary

We have investigated the magnetic properties of intrinsic as well as nitrogen and hydrogen related single and pair defects in ZnO. As a result, several of them have been found to carry a magnetic moment. Furthermore, we have shown that the magnetic moment of isolated donor-like and acceptor-like defects may be annihilated when two defects of opposing character are in the vicinity of each other. By investigating the magnetic interaction between certain defects we have found that it is essential for FM ordering that the magnetization around the defects is not completely localized at the defect site but is also distributed into the p orbitals of the host O atoms. From our results we come to the conclusion that experimentally observed hole induced magnetism in ZnO most likely originates from Zn vacancies as they show the strongest magnetic long-range interaction. This is in agreement with previous works and is also supported by Monte Carlo simulations.

Furthermore, we have shown that, by applying Hubbard- U corrections on the magnetic p orbitals, it is possible to reproduce the experimentally found localization of defect-induced holes carrying the magnetic moments. The interaction that is responsible for the magnetic ordering, however, collapses by doing so as the material becomes insulating, which is in agreement with previous works. Thus, the question of what causes the experimentally observed ferromagnetism in

ZnO remains open. Keeping in mind that DFT calculations are performed for perfectly semiconducting ZnO one might argue that the calculated interaction actually underestimates the experimental one, as in experiments at finite temperatures one usually deals with samples containing intrinsic charge carriers. The latter can possibly enhance the magnetic interaction even more. Another possible source for FM ordering in ZnO that needs further investigation is donor-like magnetic defects such as charged oxygen vacancies.

Acknowledgments

This work was financially supported by the German Research Foundation (DFG) within the SFB 762. The authors would like to thank M Khalid and P Esquinazi for many fruitful discussions.

References

- [1] Dietl T, Ohno H, Matsukura F, Cibert J and Ferrand D 2000 Zener model description of ferromagnetism in zinc-blende magnetic semiconductors *Science* **287** 1019
- [2] Pan F, Song C, Liu X J, Yang Y C and Zeng F 2008 Ferromagnetism and possible application in spintronics of transition-metal-doped ZnO films *Mater. Sci. Eng. R* **62** 1–35
- [3] Lv P, Huang F, Chu W, Lin Z, Chen D, Li W, Chen D and Wu Z 2008 Intrinsic magnetism of a series of co substituted ZnO single crystals *J. Phys.: Condens. Matter* **20** 035206
- [4] Sanchez N, Gallego S and Munoz M C 2008 Magnetic states at the oxygen surfaces of ZnO and Co-doped ZnO *Phys. Rev. Lett.* **101** 067206
- [5] Sato K *et al* 2010 First-principles theory of dilute magnetic semiconductors *Rev. Mod. Phys.* **82** 1633–90
- [6] Gacic M, Jakob G, Herbolt C, Adrian H, Tietze T, Bruck S and Goering E 2007 Magnetism of Co-doped ZnO thin films *Phys. Rev. B* **75** 205206
- [7] Hong N H, Sakai J and Virginie B 2007 Observation of ferromagnetism at room temperature in ZnO thin films *J. Phys.: Condens. Matter* **19** 036219
- [8] Ney A, Ollefs K, Ye S, Kammermeier T, Ney V, Kaspar T C, Chambers S A, Wilhelm F and Rogalev A 2008 Absence of intrinsic ferromagnetic interactions of isolated and paired co dopant atoms in $Zn_{1-x}Co_xO$ with high structural perfection *Phys. Rev. Lett.* **100** 157201
- [9] Pan H, Yi J B, Shen L, Wu R Q, Yang J H, Lin J Y, Feng Y P, Ding J, Van L H and Yin J H 2007 Room-temperature ferromagnetism in carbon-doped ZnO *Phys. Rev. Lett.* **99** 127201
- [10] Zhou S *et al* 2008 Room temperature ferromagnetism in carbon-implanted ZnO *Appl. Phys. Lett.* **93** 232507
- [11] Elfimov I S, Rusydi A, Csiszar S I, Hu Z, Hsieh H H, Lin H J, Chen C T, Liang R and Sawatzky G A 2007 Magnetizing oxides by substituting nitrogen for oxygen *Phys. Rev. Lett.* **98** 137202–4
- [12] Khalid M *et al* 2009 Defect-induced magnetic order in pure ZnO films *Phys. Rev. B* **80** 035331
- [13] Xu Q *et al* 2008 Room temperature ferromagnetism in ZnO films due to defects *Appl. Phys. Lett.* **92** 082508
- [14] Borges R P, da Silva R C, Magalhaes S, Cruz M M and Godinho M 2008 Magnetism in Ar-implanted ZnO *J. Phys.: Condens. Matter* **20** 429801
- [15] Elfimov I S, Yunoki S and Sawatzky G A 2002 Possible path to a new class of ferromagnetic and half-metallic ferromagnetic materials *Phys. Rev. Lett.* **89** 216403
- [16] Chanier T, Opahle I, Sargolzaei M, Hayn R and Lannoo M 2008 Magnetic state around cation vacancies in II–VI semiconductors *Phys. Rev. Lett.* **100** 026405
- [17] Wang Q, Sun Q, Chen G, Kawazoe Y and Jena P 2008 Vacancy-induced magnetism in ZnO thin films and nanowires *Phys. Rev. B* **77** 205411
- [18] Droghetti A, Pemmaraju C D and Sanvito S 2008 Predicting d^0 magnetism: Self-interaction correction scheme *Phys. Rev. B* **78** 140404
- [19] Pardo V and Pickett W E 2008 Magnetism from 2p states in alkaline earth monoxides: trends with varying n impurity concentration *Phys. Rev. B* **78** 134427
- [20] Máca F, Kudrnovský J, Drchal V and Bouzerar G 2008 Magnetism without magnetic impurities in ZrO_2 oxide *Appl. Phys. Lett.* **92** 212503
- [21] Coey J M D 2005 d^0 ferromagnetism *Solid State Sci.* **7** 660–7
- [22] Lany S and Zunger A 2009 Polaronic hole localization and multiple hole binding of acceptors in oxide wide-gap semiconductors *Phys. Rev. B* **80** 085202
- [23] Khalid M, Setzer A, Ziese M, Esquinazi P, Spemann D, Pöpl A and Goering E 2010 Ubiquity of ferromagnetic signals in common diamagnetic oxide crystals *Phys. Rev. B* **81** 214414
- [24] Shen L, Wu R Q, Pan H, Peng G W, Yang M, Sha Z D and Feng Y P 2008 Mechanism of ferromagnetism in nitrogen-doped ZnO: first-principle calculations *Phys. Rev. B* **78** 073306
- [25] Peng H, Xiang H J, Wei S-H, Li S-S, Xia J-B and Li J 2009 Origin and enhancement of hole-induced ferromagnetism in first-row d^0 semiconductors *Phys. Rev. Lett.* **102** 017201
- [26] Osorio-Guillen J, Lany S, Barabash S V and Zunger A 2006 Magnetism without magnetic ions: percolation, exchange, and formation energies of magnetism-promoting intrinsic defects in CaO *Phys. Rev. Lett.* **96** 107203
- [27] Wang F, Pang Z, Lin L, Fang S, Dai Y and Han S 2009 Magnetism in undoped MgO studied by density functional theory *Phys. Rev. B* **80** 144424
- [28] Wang X L, Zeng Z, Zheng X H and Lin H Q 2007 *J. Appl. Phys.* **101** 09H104
- [29] Rahman G, García-Suárez V M and Hong S C 2008 Vacancy-induced magnetism in SnO_2 : a density functional study *Phys. Rev. B* **78** 184404
- [30] Werpachowska A M and Wilamowski Z 2006 The RKKY coupling in diluted magnetic semiconductors *Mater. Sci.* **24** 675
- [31] Mahadevan P, Zunger A and Sarma D D 2004 Unusual directional dependence of exchange energies in GaAs diluted with mn: is the RKKY description relevant? *Phys. Rev. Lett.* **93** 177201
- [32] Singh A, Datta A, Das S K and Singh V A 2003 Ferromagnetism in a dilute magnetic semiconductor: generalized RKKY interaction and spin–wave excitations *Phys. Rev. B* **68** 235208
- [33] Ziener C H, Glutsch S and Bechstedt F 2004 RKKY interaction in semiconductors: effects of magnetic field and screening *Phys. Rev. B* **70** 075205
- [34] Priour D J and Das Sarma S 2006 Phase diagram of the disordered RKKY model in dilute magnetic semiconductors *Phys. Rev. Lett.* **97** 127201
- [35] McCluskey M D and Jokela S J 2009 Defects in ZnO *J. Appl. Phys.* **106** 071101
- [36] Park S Y, Shin S W, Kim P J, Kang J-H, Kim T H and Lee Y P 2007 A study on the magnetic properties of hydrogen-implanted $Zn_{0.96}Mn_{0.04}O$ films *Proc. 17th Int. Conf. on Magnetism, The Int. Conf. on Magnetism; J. Magn. Mater.* **310** e708–10
- [37] Ahn G Y, Park S-I and Kim C S 2006 Enhanced ferromagnetic properties of diluted Fe doped ZnO with hydrogen treatment *The 6th Int. Symp. on Physics of Magnetic Materials; J. Magn. Mater.* **303** e329–31
- [38] Van de Walle C G 2000 Hydrogen as a cause of doping in zinc oxide *Phys. Rev. Lett.* **85** 1012–5

- [39] Hohenberg P and Kohn W 1964 Inhomogeneous electron gas *Phys. Rev.* **136** B864–71
- [40] Kohn W and Sham L J 1965 Self-consistent equations including exchange and correlation effects *Phys. Rev.* **140** A1133–8
- [41] Perdew J P, Chevary J A, Vosko S H, Jackson K A, Pederson M R, Singh D J and Fiolhais C 1992 Atoms, molecules, solids, and surfaces: applications of the generalized gradient approximation for exchange and correlation *Phys. Rev. B* **46** 6671
- [42] Kresse G and Hafner J 1993 *Ab initio* molecular dynamics for liquid metals *Phys. Rev. B* **47** 558
- [43] Kresse G and Furthmüller J 1996 Efficiency of *ab initio* total energy calculations for metals and semiconductors using a plane-wave basis set *Comput. Mater. Sci.* **6** 15
- [44] Blöchl P E 1994 Projector augmented-wave method *Phys. Rev. B* **50** 17953
- [45] Monkhorst H J and Pack J D 1976 Special points for brillouin-zone integrations *Phys. Rev. B* **13** 5188–92
- [46] Wood D M and Zunger A 1985 A new method for diagonalising large matrices *J. Phys. A: Math. Gen.* **18** 1343–59
- [47] Yoshio K, Onodera A, Satoh H, Sakagami N and Yamashita H 2001 Crystal structure of ZnO:Li at 293 K and 19 K by x-ray diffraction *Ferroelectrics* **264** 133
- [48] Janotti A and Van de Walle C G 2007 Native point defects in ZnO *Phys. Rev. B* **76** 165202
- [49] Tuomisto F, Saarinen K, Look D C and Farlow G C 2005 Introduction and recovery of point defects in electron-irradiated ZnO *Phys. Rev. B* **72** 085206
- [50] Fischer G, Däne M, Ernst A, Bruno P, Lüders M, Szotek Z, Temmerman W and Hergert W 2009 Exchange coupling in transition metal monoxides: electronic structure calculations *Phys. Rev. B* **80** 014408
- [51] Binder K 1981 Finite size scaling analysis of ising model block distribution functions *Z. Phys. E* **43** 361
- [52] Jokela S J and McCluskey M D 2007 Unambiguous identification of nitrogen–hydrogen complexes in ZnO *Phys. Rev. B* **76** 193201
- [53] Li X, Keyes B, Asher S, Zhang S B, Wei S-H, Coutts T J, Limpijumnong S and Van de Walle C G 2005 Hydrogen passivation effect in nitrogen-doped ZnO thin films *Appl. Phys. Lett.* **86** 122107
- [54] Sokol A A, French S A, Bromley S T, Catlow C R A, van Dam H J J and Sherwood P 2007 Point defects in ZnO *Faraday Discuss.* **134** 267
- [55] Brauer G *et al* 2009 Identification of Zn-vacancy–hydrogen complexes in ZnO single crystals: a challenge to positron annihilation spectroscopy *Phys. Rev. B* **79** 115212
- [56] Chan J A, Lany S and Zunger A 2009 Electronic correlation in anion p orbitals impedes ferromagnetism due to cation vacancies in Zn chalcogenides *Phys. Rev. Lett.* **103** 016404